

One-Step Synthesis of Methylene Blue-Encapsulated Zeolitic Imidazolate Framework for Dual-Signal Fluorescent and Homogeneous Electrochemical Biosensing

Jiafu Chang, Wenxin Lv, Qian Li, Haiyin Li,* and Feng Li*

Cite This: *Anal. Chem.* 2020, 92, 8959–8964

Read Online

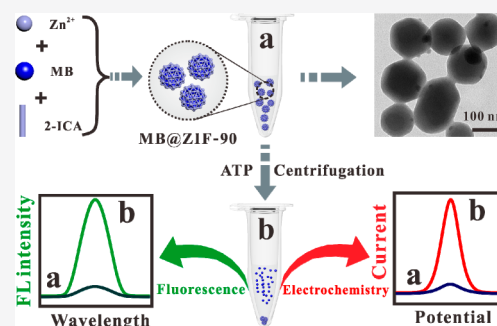
ACCESS |

Metrics & More

Article Recommendations

Supporting Information

ABSTRACT: In vitro diagnosis requires target biomarkers to be reliably detected at an ultralow level. A dual-signal strategy permits self-calibration to overcome the interferences of experimental and environmental factors, and thus is regarded as a promising approach. However, currently reported works mainly concentrated on the same forms of energy of output signals. Herein, we propose a one-step strategy for synthesis of methylene blue-encapsulated zeolitic imidazolate framework-90 (MB@ZIF-90) with high loading, unique dual-signal property, exceptional recognition capability, and good stability, and we further pioneer MB@ZIF-90 as a dual-signal biosensor for label-free, enzyme-free, and ultrasensitive detection of adenosine triphosphate (ATP) by integration of fluorescence and homogeneous electrochemical techniques. The recognition of MB@ZIF-90 by target ATP spurs the decomposition of ZIF-90, subsequently permitting MB to be released into a supernatant. As compared to the case where ATP does not exist, obviously increased intensities in fluorescence and differential pulse voltammetry current are observed and both signals are directly proportional to ATP concentrations. Thus, the MB@ZIF-90-based biosensor achieved dual-signal detection of ATP in an ultrasensitive manner and displayed a more reliable diagnosis result than previously reported ATP biosensors. This dual-signal strategy provides a new opportunity to develop high-performance biosensors for in vitro diagnosis and demonstrates great potential for future applications in bioinformatics and clinical medicine.



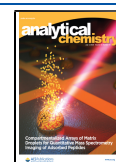
Biomarkers are important biochemical indicators, are closely connected with the variation in structure and function of organisms, cells, and subcells, and features a higher level of sensitivity than imaging and symptoms.^{1,2} In this context, the development of high-performance biomarker assays is very meaningful for the field of bioinformatics and clinical medicine, and will provide more important information for accurate diagnosis of various diseases.^{3,4} However, the expression level of most biomarkers in biological fluids is ultralow and the fluid environments are complex,⁵ which are detrimental to efficient and reliable identification of biomarkers. Many techniques including fluorescence detection,^{6–8} electrochemical sensing,^{9–11} surface-enhanced Raman scattering (SERS),^{12–14} and others have been explored for diverse biomarkers sensitive biosensing based on an enzyme-assisted amplification strategy.^{15–17} For example, Yuan's group reported an enzyme-assisted cascade catalytic reaction for ultrasensitive electrochemical detection of genes.¹⁸ Nevertheless, no matter what the technique, they detect target objects on the basis of the variation in a single signal. A single-signal readout easily leads to inaccuracy because of the effect of nonstandard test administration, different operators, and different experimental environments. In contrast, dual signals can obviously improve the diagnosis accuracy because of their

self-calibration function, and such a dual-signal strategy has attracted the interest of many researchers.^{19–21} However, the dual signals of reported biosensors belong to the same forms of energy, which inevitably result in a relatively high background noise. It is profitable to construct a dual-signal platform that has different forms of energy and can achieve the output of dual signals in a single assay without the addition of other reagents; however, no simple example for developing such a dual-signal biosensor has been proposed, especially for electrochemical and fluorescence signals. Homogeneous electrochemical biosensors, a subclass of electrochemical biosensors, generate different pulse voltammetry (DPV) signals through the diffusion of electroactive dyes toward electrodes without immobilization of biorecognizable units, and thus they possess the advantages of simplicity, rapidity, sensitivity, and low price and have attracted a great deal of interest from analytical scientists in the fields of disease

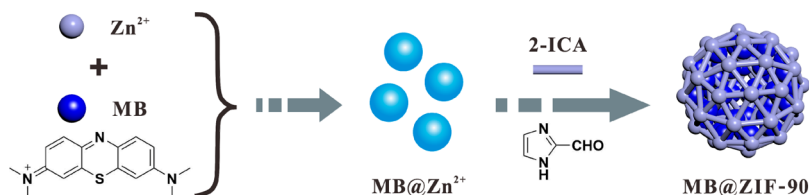
Received: March 3, 2020

Accepted: June 1, 2020

Published: June 1, 2020



Scheme 1. Schematic Diagram of One-Step Synthesis of MB@ZIF-90



diagnosis, food safety, and environmental protection.^{3,19,22} On the other hand, fluorescence biosensors have applied light as an output signal and have more than $\sim 10^3$ times increase in sensitivity than colorimetric assays.^{23–25} More importantly, the energy form of light is greatly different from that of homogeneous electrochemical biosensors. If homogeneous electrochemical and fluorescence techniques were integrated together, a brand-new dual-signal biosensor for higher efficiency and more accurate diagnosis of biomarkers will be successfully developed.

Adenosine triphosphate (ATP) is a natural nucleotide consisting of one adenine, one ribose, and three phosphate groups and is a potential biomarker for evaluating cell proliferation and death.²⁶ Abnormal expression of ATP in the human body is broadly regarded to indicate risk of angiocardopathy, Parkinson's disease, and Alzheimer's disease.^{27–29} In addition, it is reported that the expression level of ATP in brain, serum, and other body fluids is extremely low.³⁰ Given the above information, substantial efforts have been devoted to the development of high-performance ATP biosensors.^{31–33} Despite great progress, it is noteworthy that previous ATP biosensors face the following obstacles: First, most ATP biosensors devote themselves to a single signal, and others have dual signals but have the same energy forms. Second, most ATP biosensors are developed on the basis of the aptamer technique, which suffered from the strict design of deoxyribonucleic acid (DNA) probes and a high-cost/complicated labeling procedure. Third, they require bioenzymes to enhance the detection sensitivity and, thus, fail to obtain a rapid response and achieve low cost. For resolving the problems mentioned above, we strive, here, to develop a label-free, enzyme-free, and dual-signal biosensor for ATP ultrasensitive and accurate biosensing by coupling fluorescence and homogeneous electrochemical techniques.

Zeolitic imidazolate framework-90 (ZIF-90) is a porous and biocompatible metal–organic framework (MOF) built from Zn^{2+} and imidazolate-2-carboxyaldehyde (2-ICA), possesses large surface area and pore size, and is an excellent nanocarrier for encapsulating molecules.^{34–36} The procedure for encapsulation generally includes the following steps: First, ZIF-90 preparation; second, ZIF-90 drying and cleanup of solvent molecules; third, loading of molecules in pores; fourth, sealing off the pores, which are complex and costly, resulting in low loading and poorly controlled release and production of abundant waste.^{37,38} At the same time, the diameters of its pore opening and pore cavity are small, and thus relatively large substances cannot be encapsulated inside ZIF-90.³⁹ A method to address these obstacles is to introduce ZIF-90 preparation and molecule encapsulation into a one-step operation. Such molecule-encapsulated ZIF-90 composites not only avoid the complicated preparation steps but also increase the loading, enhance the controlled release, and allow the encapsulation of large molecules.^{36,40,41} If we introduce a molecule-encapsulated ZIF-90 composite into a ATP bio-

sensor and regulate the loading molecules, such a proposed biosensor would realize the label-free, enzyme-free, ultrasensitive, and dual-signal detection of ATP.

Herein, we prepared a methylene blue-encapsulated ZIF-90 (MB@ZIF-90) through combining the fabrication of ZIF-90 and encapsulation of MB in a one-step reaction in which ZIF-90 and MB were applied as the affinity material and signal source, respectively. Experimental measurements demonstrated that MB was effectively encapsulated inside ZIF-90, and the prepared MB@ZIF-90 possessed high stability under physiological conditions. We further pioneered that MB@ZIF-90 is a promising ATP-responsive dual-signal biosensor because of the competitive coordination between ATP and 2-ICA on Zn^{2+} . Because of ZIF-90s high loading and unique recognition capability on ATP, and the excellent dual-signal property of MB, ultrasensitive and dual-signal detection of ATP with label-free and enzyme-free features was realized.

EXPERIMENTAL SECTION

Synthesis of MB@ZIF-90. Four milliliters of *N,N*-dimethylformamide (DMF) containing 0.0439 g of $\text{Zn}(\text{CH}_3\text{COOH})_2 \cdot 2\text{H}_2\text{O}$ and 0.0013 g of MB was stirred for 15 min. After that, 6.0 mL of DMF containing 0.038 g of 2-ICA was added, and the final solution reacted for 15 min. Through centrifugation and successive washing with DMF, ultrapure water, and ethanol three times, respectively, MB@ZIF-90 was obtained. For ZIF-90, the preparation process is the same as that of MB@ZIF-90. MB@ZIF-90 was dispersed in HEPES buffer (10 mM, pH 7.4) to get a 10 mg/mL stock solution.

Dual-Signal Detection of ATP Based on MB@ZIF-90. Two hundred microliters of HEPES buffer containing 1.0 mg/mL MB@ZIF-90 and target ATP with different amounts was incubated for 5.0 min. The reaction solution was then centrifuged at 10000 rpm for 1.0 min and the supernatant was exposed to fluorescence and DPV characterizations.

RESULTS AND DISCUSSION

Synthesis and Characterization of MB@ZIF-90. The illustration for one-step synthesis of MB@ZIF-90 is manifested in Scheme 1. MB has N and S elements that possess weak coordination interaction with metal ions, and thus MB reacts with Zn^{2+} to form a coordination intermediate (MB@Zn^{2+}). 2-ICA was added to competitively chelate with Zn^{2+} in MB@Zn^{2+} and then ZIF-90 was prepared. Along with the formation of ZIF-90, MB was successfully encapsulated. For validation of the formation of MB@ZIF-90, the identity and phase purity were characterized by X-ray diffraction (XRD) (Figure 1A). The peaks of MB@ZIF-90 in the range of 5° – 40° were sharp and were in line with that of prepared ZIF-90 and simulated ZIF-90 single crystal. Besides, there were no unwanted peaks of MB observed. These observations obviously demonstrated that MB@ZIF-90 was of good purity and high crystallinity, that MB was encapsulated inside ZIF-90 rather than being physically

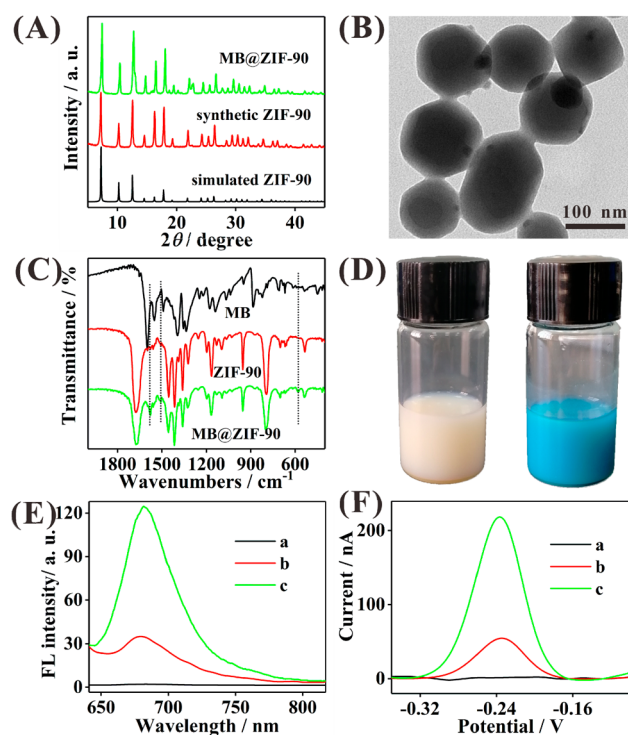


Figure 1. (A) XRD patterns of simulated ZIF-90, synthetic ZIF-90, and MB@ZIF-90. (B) TEM image of MB@ZIF-90. (C) FT-IR spectra of MB, ZIF-90, and MB@ZIF-90. (D) Images of ZIF-90 (left) and MB@ZIF-90 (right) dispersed in water solution. Fluorescence spectra (E) and DPV curves (F) of ZIF-90 (a), MB@ZIF-90 (b), and MB (c).

adsorbed on the surface, and that the encapsulated MB had a minor influence on ZIF-90's lattice distortion. Transmission electron microscopy (TEM) characterization depicted that MB@ZIF-90 exhibited a uniformly dispersed nanospherical morphology (Figure 1B), and its diameter was determined to be 120 nm. For further confirmation of the loading of MB inside ZIF-90, Fourier transform infrared spectroscopy (FT-IR) characterizations were carried out (Figure 1C). In comparison to ZIF-90, MB@ZIF-90 displayed new peaks at 1581, 1507, and 576 cm^{-1} , which were attributable to MB. Along with the emergence of new FT-IR peaks, the color of MB@ZIF-90 solution changed from white into blue (Figure 1D).

Fluorescent and DPV techniques were conducted for MB, ZIF-90, and MB@ZIF-90, individually (Figure 1E,F), to gain more information about the preparation of MB@ZIF-90 and to disclose MB's dual-signal property. For ZIF-90 and MB@ZIF-90, DPV characterizations were performed by dropping them on indium tin oxide (ITO) electrode to prepare ZIF-90/ITO and MB@ZIF-90/ITO electrodes, respectively. The others were carried out in a homogeneous solution. It is important to note that MB emitted strong fluorescence at 683 nm under the excitation of 610 nm light and displayed a significant oxidation peak at -0.23 V. Supporting this notion, MB was a good dual-signal source and enabled us to achieve the dual-signal fluorescence and homogeneous electrochemical detection of ATP in a single assay. In contrast, the FL intensity at 683 nm and peak current at -0.23 V of ZIF-90 were extremely low. It came as no surprise that no MB existed inside ZIF-90 and the signal intensities were dependent on the

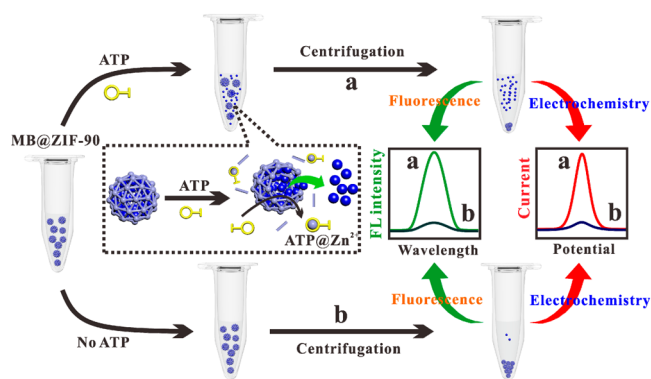
amount of MB. In this context, MB@ZIF-90 exhibited higher FL intensity and peak current than ZIF-90. This information revealed that MB was surely loaded inside ZIF-90 and had unprecedented dual-signal property.

In view of the effect of stability on diagnosis results, we challenged MB@ZIF-90 by placing it in a reaction buffer containing glucose, bovine serum albumin (BSA), histidine, dopamine, and a 10-fold diluted serum sample, respectively, and the supernatants obtained through centrifugation were characterized by fluorescence and DPV techniques. As illustrated in Figure S1A (Supporting Information), whether the FL intensity or peak current, they both maintained slight changes, even if the incubation time increased to 36 h, and thus MB@ZIF-90 was stable. Expectedly, no changes in the TEM image (Figure S1B) and XRD pattern (Figure S1C) were observed compared with that of untreated MB@ZIF-90. Moreover, FL intensity and peak current were also very low when MB@ZIF-90 existed in the serum sample, justifying its sufficient stability for practical application (Figure S1D). Furthermore, MB@ZIF-90 was dispersed into different pH solutions for 36 h to assess its response to the pH value (Figure S2). Both fluorescence and electrochemical signals were low in the pH range of 4.0–11, which implied no leakage of MB, suggesting high pH stability. When the pH value was larger than 11 or smaller than 4.0, the FL intensity and peak current elevated abruptly, indicating the release of MB and MB@ZIF-90's weak stability in strong acid and base solutions. Meanwhile, the released MB made us be once more sure that MB was effectively loaded inside ZIF-90.

Sensing Principle of MB@ZIF-90-Based Biosensor.

Given the above-mentioned characteristics, we deduced that MB@ZIF-90 was competent for label-free, enzyme-free, and dual-signal detection of ATP in an ultra-high-sensitivity manner, and the detailed principle was illustrated in Scheme 2. When ATP was absent, MB@ZIF-90 maintained its

Scheme 2. Schematic Representation of MB@ZIF-90-Based Biosensor for Ultrasensitive and Dual-Signal Detection of ATP



structure and morphology with minor variation, and the unspoiled ZIF-90 prohibited the release of MB. As a result, no or only small MB was observed in the supernatant, and the detected fluorescence and DPV signals were very low. However, upon the addition of ATP, it decomposed ZIF-90 due to the fact that the phosphate group and adenosine group in ATP have stronger coordination with Zn^{2+} than the iminazole group in 2-ICA,³⁶ subsequently leading to the collapse of the ZIF-90 framework and permitting the release of

MB from ZIF-90 into solution. Thus, a large diversity of MB was determined in a supernatant and contributed to both high FL intensity and DPV current because of its unique dual-signal property. Considering both of the increased signals, a MB@ZIF-90-based dual-signal biosensor for label-free, enzyme-free, and ultrasensitive detection of ATP was developed on the basis of the integration of fluorescence and homogeneous electrochemical techniques.

Assay Feasibility of MB@ZIF-90-Based Biosensor. For investigation of the feasibility of a MB@ZIF-90-based biosensor for ATP assay, reaction solutions that have or do not have ATP were exposed to fluorescence and DPV measurements (Figure 2A,B). If ATP was absent, the FL

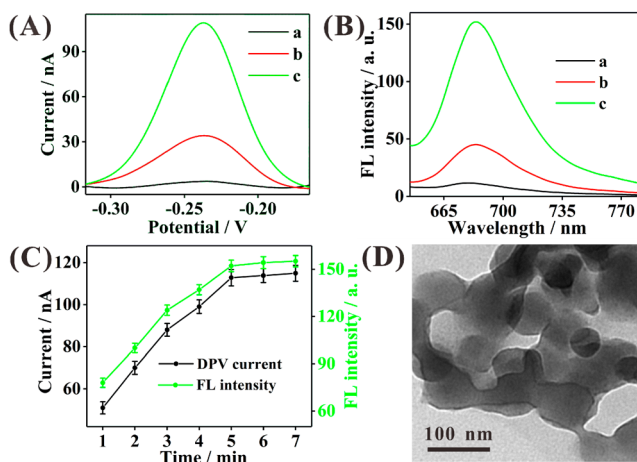


Figure 2. DPV (A) and fluorescence (B) curves of supernatant in the presence of ATP with different amounts: (a) 0, (b) 20, and (c) 100 nM. (C) FL intensity and DPV current versus reaction time between MB@ZIF-90 and ATP. (D) TEM image of MB@ZIF-90 after the reaction with 100 nM ATP for 2 min.

intensity and DPV current of MB were only 12.02 au and 4.13 nA, respectively. Nevertheless, upon the addition of ATP, the supernatant displayed significantly increased fluorescence and electrochemical signals up to 45.00 au and 34.00 nA, respectively. It might be attributable to the fact that large-scale MB was released into the supernatant upon the selective decomposition of ZIF-90 by ATP, thereby leading to enhancement in FL intensity and DPV current. Moreover, both signals further increased along with the increasing amount of ATP, demonstrating a definite positive relationship between signal intensity and ATP concentration. This is because more ATP disassembles more ZIF-90 to release more MB into the supernatant. Meanwhile, the response time required only 5 min (Figure 2C), to the best of our knowledge, which is the shortest time to complete the detection of ATP. Both increased signals obviously suggested that label-free, enzyme-free, ultrasensitive and dual-signal detection of ATP could be readily realized using MB@ZIF-90-based biosensor.

Furthermore, UV-vis and TEM techniques were successively employed to characterize the release of MB and the collapse of MB@ZIF-90. The UV-vis curves in Figure S3 reveal that the supernatant in the presence of ATP possessed two new peaks at 612 and 663 nm (which were assigned to MB) compared to that in the absence of ATP, validating the ATP-initiated efficient release of MB from MB@ZIF-90 too. Besides, after the addition of 100 nM ATP for 2.0 min, MB@ZIF-90 exhibited an irregular aggregation morphology rather

than homogeneous nanospheres (Figure 2D), which might be understood in terms of the ATP having stronger coordination with Zn^{2+} than 2-ICA, further damaging ZIF-90, accompanied by the release of MB.

For investigation of such an ATP-responsive fluorescence and DPV current turn-on phenomenon, competitive interaction between ATP and 2-ICA on Zn^{2+} was examined. The experiment was proposed by prereaction of ATP and adenosine triphosphatase (ATPase) and subsequent addition of MB@ZIF-90 (Figure S4A). ATPase-catalyzed hydrolysis of ATP into adenosine diphosphate (ADP), which does not have a stronger coordination interaction with Zn^{2+} than 2-ICA, leading to no release of MB. Therefore, the FL intensity and DPV current of MB in supernatant were very low. As illustrated in Figure S4B, in comparison to the case where ATPase did not exist, the prereaction of ATPase with ATP resulted in both low fluorescence and electrochemical signals that are about identical to those of individual MB@ZIF-90, obtained from the high catalyzing efficiency of ATPase toward ATP and subsequent vanishing of ATP-initiated collapse of MB@ZIF-90.

Analytical Performance of MB@ZIF-90-Based Biosensor. For evaluation of the sensing ability of a MB@ZIF-90-based biosensor for ultrasensitive and dual-signal detection of ATP, an array of solutions containing ATP with different concentrations were exposed to fluorescence and electrochemical measurements. As depicted in Figure 3A,C, the

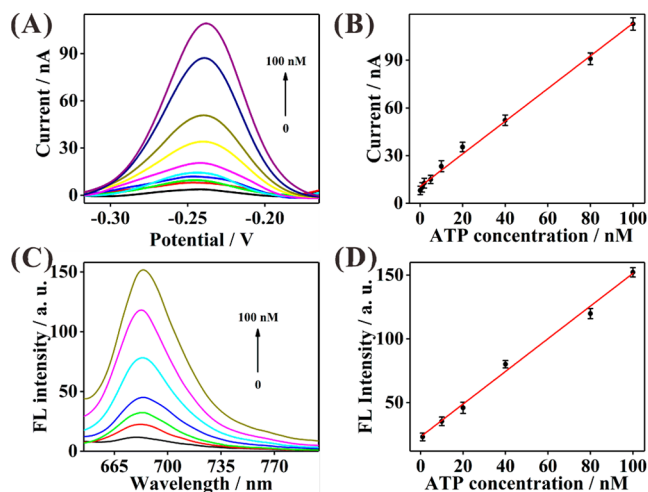


Figure 3. (A) DPV responses of supernatant upon the addition of ATP with different concentrations: 0, 0.1, 1, 2, 5, 10, 20, 40, 80, and 100 nM. (B) Linear relationship between the current and ATP concentration. (C) Fluorescence spectra of the supernatant upon the addition of ATP with different concentrations: 0, 1, 10, 20, 40, 80, and 100 nM. (D) Linear relationship between FL intensity and ATP concentration.

fluorescence and current responses of MB elevated, along with the increase in ATP concentrations, displaying a directly positive relationship between signal intensity and amount of ATP. Calibration plots were further obtained through application of the FL intensity (F) and peak current (I) as vertical coordinates and ATP concentrations (C_{ATP}) from 1 to 100 nM and 0.1 to 100 nM as horizontal coordinates, respectively. They demonstrated a high linearity with coefficients of 0.9950 and 0.9919 (Figure 3B,D), and the equations were determined to be $F = 1.28C_{\text{ATP}} + 23.205$ and I

$= 1.0275C_{\text{ATP}} + 10.4905$. The detection limits reached 0.38 nM with the fluorescence technique and 0.027 nM for the homogeneous electrochemical technique based on 3σ , respectively, and were compared to those of other methods in Table S1. Obviously, the detection limit was comparable to or smaller than those of previously reported probes that focused on single-signal determination of ATP based on the aptamer strategy, being governed by a complex and high-cost labeling process, strict design of DNA sequences, and expensive bioenzymes. This high performance may result from ZIF-90's porous structure and one-step preparation strategy, enabling the encapsulation of a large diversity of MB, and exceptional recognition capability of ZIF-90 on ATP, permitting a significant increase in the concentration of released MB upon the addition of only a small amount of ATP. Overall, this MB@ZIF-90-based biosensor possessed apparent advantages of simple operation, fast analysis, and low price, and therefore it was regarded as a more popular tool for ultrasensitive and dual-signal analysis of ATP, favoring the rapid, early, and accurate diagnosis of ATP-related diseases.

Selectivity, Stability, and Precision. ADP, adenosine monophosphate (AMP), and pyrophosphate (PPi), which have similar structures to ATP, and glucose, BSA, histidine, and dopamine, which may coexist with ATP in biological samples, were applied as interfering molecules to examine the selectivity and anti-interference ability of the MB@ZIF-90-based biosensor (Figure 4A). The ΔI ($\Delta I = I_{\text{ATP}} - I_0$, where

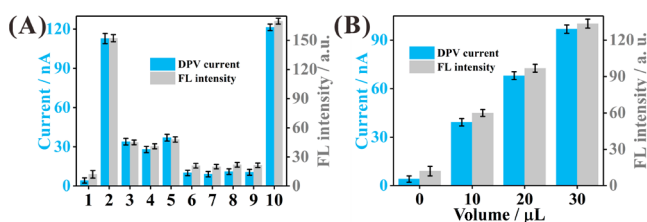


Figure 4. (A) Selectivity experiment of the MB@ZIF-90-based biosensor for ATP: (1) blank, (2) ATP, (3) ADP, (4) AMP, (5) PPi, (6) glucose, (7) histidine, (8) dopamine, (9) BSA, and (10) mixture. (B) FL intensity and DPV current of a MB@ZIF-90-based biosensor corresponding to different volumes of MCF cell lysis solution: 0, 10, 20, and 30 μL . The total detection volume was 200 μL .

I_{ATP} is the current of the supernatant in the presence of ATP and I_0 is the current of supernatant in the absence of ATP) and ΔF ($\Delta F = F_{\text{ATP}} - F_0$, where F_{ATP} is the FL intensity of supernatant in the presence of ATP and F_0 is the FL intensity of supernatant in the absence of ATP) of ATP was 3.6 and 4.24, 4.5 and 4.82, 3.27 and 3.88, 18.21 and 15.5, 21.62 and 17.5, 15.43 and 14.35, and 16.61 and 14.73 times higher than that of ADP, AMP, PPi, glucose, BSA, histidine, and dopamine, respectively. Furthermore, it was revealed that the variations in FL intensity and DPV current of MB in the presence of ATP and the interferences were only 17.6 au and 8.6 nA compared to that in the presence of ATP alone, undoubtedly implying that the MB@ZIF-90-based biosensor had distinguished specificity for discriminating ATP against other matters, especially ADP and AMP, and strong anti-interference ability. The stability of this biosensor was tested by keeping MB@ZIF-90 in a dark environment at 4 $^{\circ}\text{C}$ for 36 h, and subsequently this sensor was employed to detect 100 nM ATP. Both detected fluorescence and electrochemical signals maintained 103.7% and 105.1% of that obtained from untreated MB@ZIF-

90, justifying the high stability (Figure S5A). Furthermore, the interassay precision of the proposed biosensor was studied through employing six differently prepared MB@ZIF-90s in the analysis of 100 nM ATP (Figure S5B). The calculated relative standard deviations (RSDs) were around 4.3% and 3.7% for fluorescence and electrochemical techniques, respectively, indicating an acceptable fabrication repeatability.

Real Sample Analysis. For testing of the applicability of the MB@ZIF-90-based biosensor for ATP in a clinical sample, recovery experiments were first conducted by spiking ATP with different amounts into diluted human serum samples (Table S2). The recoveries were calculated to be 102.1% (101.7%), 102.15% (98.95%), and 101.36% (102.24%) for the assay of 10, 20, and 50 nM ATP, and the RSDs were around 3.32% (3.25%), 3.62% (3.17%), and 2.93% (3.37%), respectively. The acceptable recoveries and low RSDs suggested good reproducibility. Furthermore, the MB@ZIF-90-based biosensor was employed to detect ATP in MCF-7 cell lysis solution at a density of 1.0×10^6 cells/mL. The MCF-7 cell lysis solution was diluted with a HEPES buffer before analysis. It can be clearly seen from Figure 4B that, with increasing volume of the lysis solution, the resultant solution displayed gradually increasing fluorescence and DPV signals. Through the change in FL intensity and DPV current, the expression level of ATP in the MCF-7 cell lysis solution was determined to be 5.63 mM using the fluorescence technique and 5.75 mM using the homogeneous electrochemical technique, which were in good agreement with those of previously reported methods.⁴²

CONCLUSIONS

In summary, we proposed a one-step strategy for preparation of MB-encapsulated ZIF-90 (MB@ZIF-90) with high loading, unique dual-signal property, and splendid stability, and we have also displayed its application in the development of a label-free, enzyme-free, ultrasensitive, and dual-signal biosensor, using ATP as the proof-of-concept analyte. Compared to previously reported ATP biosensors, the MB@ZIF-90-based biosensor had several advantages: First, this is the first developed dual-signal biosensor for ATP assay with different energy forms. Second, it fully utilizes the high loading of ZIF-90 toward MB and has exceptional recognition capability of ZIF-90 on ATP to achieve ATP biosensing with a low detection limit and the shortest detection time. Third, it abandons DNA probes and bioenzymes and possesses the advantages of simple operation and low cost. Moreover, this promising strategy is also applicable to other functional molecules and opens up a new path for developing dual-signal biosensors, thus providing a promising approach for more accurate diagnosis of ATP-related diseases.

ASSOCIATED CONTENT

Supporting Information

The Supporting Information is available free of charge at <https://pubs.acs.org/doi/10.1021/acs.analchem.0c00952>.

Reagents and materials, apparatus, ATP assay performance of our strategy and other methods, recoveries and RSDs of the proposed biosensor for ATP spiked in serum samples, stability of synthesized MB@ZIF-90, FL intensity and DPV current of supernatant versus different pH values, UV-vis absorption spectra, interaction of ATPase, ATP, and MB@ZIF-90, stability

and repeatability investigation of the biosensor, and additional references (PDF)

AUTHOR INFORMATION

Corresponding Authors

Feng Li – College of Chemistry and Pharmaceutical Sciences, Qingdao Agricultural University, Qingdao 266109, People's Republic of China; College of Chemistry, Chemical Engineering and Materials Science, Shandong Normal University, Jinan 250014, People's Republic of China; orcid.org/0000-0002-3894-6139; Phone: 86-532-58957855; Email: lifeng@qau.edu.cn

Haiyin Li – College of Chemistry and Pharmaceutical Sciences, Qingdao Agricultural University, Qingdao 266109, People's Republic of China; Email: lihaiyin@qau.edu.cn

Authors

Jiafu Chang – College of Chemistry and Pharmaceutical Sciences, Qingdao Agricultural University, Qingdao 266109, People's Republic of China; College of Chemistry, Chemical Engineering and Materials Science, Shandong Normal University, Jinan 250014, People's Republic of China

Wenxin Lv – College of Chemistry and Pharmaceutical Sciences, Qingdao Agricultural University, Qingdao 266109, People's Republic of China

Qian Li – College of Chemistry and Pharmaceutical Sciences, Qingdao Agricultural University, Qingdao 266109, People's Republic of China

Complete contact information is available at:

<https://pubs.acs.org/10.1021/acs.analchem.0c00952>

Notes

The authors declare no competing financial interest.

ACKNOWLEDGMENTS

This work was financially supported by the National Natural Science Foundation of China (21605093 and 21775082), the Shandong Province Higher Educational Program for Young Innovation Talents, the Major Program of Shandong Province Natural Science Foundation (ZR2018ZC0127), and the Special Foundation for Distinguished Taishan Scholar of Shandong Province (ts201511052).

REFERENCES

- (1) Sawyers, C. L. *Nature* **2008**, 452, 548–552.
- (2) Sapra, R.; Verma, R. P.; Maurya, G. P.; Dhawan, S.; Babu, J.; Haridas, V. *Chem. Rev.* **2019**, 119, 11391–11441.
- (3) Chang, J. F.; Wang, X.; Wang, J.; Li, H. Y.; Li, F. *Anal. Chem.* **2019**, 91, 3604–3610.
- (4) Bock, C.; Halbritter, F.; Carmona, F. J.; Tierling, S.; Datlinger, P.; Assenov, Y.; Berdasco, M.; Bergmann, A. K.; Booher, K.; Busato, F.; Campan, M.; Dahl, C.; Dahmcke, C. M.; Diep, D.; Fernández, A. F.; Gerhauser, C.; Haake, A.; Heilmann, K.; Holcomb, T.; Hussmann, D.; et al. *Nat. Biotechnol.* **2016**, 34, 726–737.
- (5) Shi, J.; Deng, Q. C.; Wan, C. Y.; Zheng, M. M.; Huang, F. H.; Tang, B. *Chem. Sci.* **2017**, 8, 6188–6195.
- (6) Li, P. X.; Wei, M.; Zhang, F.; Su, J.; Wei, W.; Zhang, Y. J.; Liu, S. Q. *ACS Appl. Mater. Interfaces* **2018**, 10, 43405–43410.
- (7) Tang, X.; Deng, R. J.; Sun, Y. P.; Ren, X. J.; Zhou, M. X.; Li, J. H. *Anal. Chem.* **2018**, 90, 10001–10008.
- (8) Miao, X. M.; Cheng, Z. Y.; Ma, H. Y.; Li, Z. B.; Xue, N.; Wang, P. *Anal. Chem.* **2018**, 90, 1098–1103.
- (9) Koo, K. M.; Carrascosa, L. G.; Trau, M. *Nano Res.* **2018**, 11, 940–952.
- (10) Deng, L.; Wu, Y. H.; Xu, S. X.; Tang, Y. R.; Zhang, X. F.; Wu, P. *ACS Sensors* **2018**, 3, 1190–1195.
- (11) Qin, X. L.; Dong, Y. F.; Wang, M. H.; Zhu, Z. W.; Li, M. X.; Chen, X. J.; Yang, D.; Shao, Y. H. *Sci. China: Chem.* **2018**, 61, 476–482.
- (12) Lenzi, E.; Jimenez de Aberasturi, D.; Liz-Marzán, L. M. *ACS Sensors* **2019**, 4, 1126–1137.
- (13) Saleh, T. A.; Al-Shalalfeh, M. M.; Al-Saadi, A. A. *Sens. Actuators, B* **2018**, 254, 1110–1117.
- (14) Lee, T.; Wi, J.-S.; Oh, A.; Na, H.-K.; Lee, J.; Lee, K.; Lee, T. G.; Haam, S. *Nanoscale* **2018**, 10, 3680–3687.
- (15) Wang, M. H.; Yin, H. S.; Zhou, Y. L.; Meng, X. J.; Waterhouse, G. I. N.; Ai, S. Y. *Chem. Eng. J.* **2019**, 365, 351–357.
- (16) Qiu, Z.; Shu, J.; Tang, D. P. *Anal. Chem.* **2018**, 90, 1021–1028.
- (17) Rashidani, J.; Kamali, M.; Sedighian, H.; Akbariomi, M.; Mansouri, M.; Kooshki, H. *Biosens. Bioelectron.* **2018**, 102, 226–233.
- (18) Wang, D.; Chai, Y. Q.; Yuan, Y. L.; Yuan, R. *Anal. Chem.* **2019**, 91, 3561–3566.
- (19) Chang, J. F.; Li, H. Y.; Li, F. *Chem. Commun.* **2019**, 55, 10603–10606.
- (20) Wang, H.; Pu, G. Q.; Devaramani, S.; Wang, Y. F.; Yang, Z. F.; Li, L. F.; Ma, X. F.; Lu, X. Q. *Anal. Chem.* **2018**, 90, 4871–4877.
- (21) Cai, X.-L.; Zheng, B.; Zhou, Y.; Younis, M. R.; Wang, F.-B.; Zhang, W.-M.; Zhou, Y.-G.; Xia, X.-H. *Chem. Sci.* **2018**, 9, 6080–6084.
- (22) Fu, C. L.; Liu, C.; Li, Y.; Guo, Y. J.; Luo, F.; Wang, P. L.; Guo, L. H.; Qiu, B.; Lin, Z. Y. *Anal. Chem.* **2016**, 88, 10176–10182.
- (23) Greenwald, E. C.; Mehta, S.; Zhang, J. *Chem. Rev.* **2018**, 118, 11707–11794.
- (24) Lau, D.; Walsh, J. C.; Peng, W.; Shah, V. B.; Turville, S.; Jacques, D. A.; Böcking, T. *ACS Appl. Mater. Interfaces* **2019**, 11, 34586–34594.
- (25) Capilli, G.; Cavallera, S.; Anfossi, L.; Giovannoli, C.; Minella, M.; Baggiani, C.; Minero, C. *Nano Res.* **2019**, 12, 1862–1870.
- (26) Liu, Z. C.; Wu, P. C.; Yin, Y. Y.; Tian, Y. *Chem. Commun.* **2019**, 55, 9955–9958.
- (27) Li, S.; Zhao, X. T.; Yu, X. X.; Wan, Y. Q.; Yin, M. Y.; Zhang, W. W.; Cao, B. Q.; Wang, H. *Anal. Chem.* **2019**, 91, 14737–14742.
- (28) Li, X.; Yang, J. M.; Xie, J. Q.; Jiang, B. Y.; Yuan, R.; Xiang, Y. *Biosens. Bioelectron.* **2018**, 102, 296–300.
- (29) Tan, K.-Y.; Li, C.-Y.; Li, Y.-F.; Fei, J. J.; Yang, B.; Fu, Y.-J.; Li, F. *Anal. Chem.* **2017**, 89, 1749–1756.
- (30) Zhang, K. L.; He, X. L.; Liu, Y.; Yu, P.; Fei, J. J.; Mao, L. Q. *Anal. Chem.* **2017**, 89, 6794–6799.
- (31) Lu, L.; Si, J. C.; Gao, Z. F.; Zhang, Y.; Lei, J. L.; Luo, H. Q.; Li, N. B. *Biosens. Bioelectron.* **2015**, 63, 14–20.
- (32) Fan, Y.-Y.; Mou, Z.-L.; Wang, M.; Li, J.; Zhang, J.; Dang, F.-Q.; Zhang, Z.-Q. *Anal. Chem.* **2018**, 90, 13708–13713.
- (33) Xu, Y. Y.; Xu, J.; Xiang, Y.; Yuan, R.; Chai, Y. Q. *Biosens. Bioelectron.* **2014**, 51, 293–296.
- (34) Morris, W.; Doonan, C. J.; Furukawa, H.; Banerjee, R.; Yaghi, O. M. J. *Am. Chem. Soc.* **2008**, 130, 12626–12627.
- (35) Brown, A. J.; Johnson, J. R.; Lydon, M. E.; Koros, W. J.; Jones, C. W.; Nair, S. *Angew. Chem., Int. Ed.* **2012**, 51, 10615–10618.
- (36) Deng, J. J.; Wang, K.; Wang, M.; Yu, P.; Mao, L. Q. *J. Am. Chem. Soc.* **2017**, 139, 5877–5882.
- (37) Kahn, J. S.; Freage, L.; Enkin, N.; Garcia, M. A. A.; Willner, I. *Adv. Mater.* **2017**, 29, 1602782.
- (38) Wu, S.; Li, C.; Shi, H.; Huang, Y.; Li, G. X. *Anal. Chem.* **2018**, 90, 9929–9935.
- (39) Zheng, H. Q.; Zhang, Y. N.; Liu, L. F.; Wan, W.; Guo, P.; Nyström, A. M.; Zou, X. D. *J. Am. Chem. Soc.* **2016**, 138, 962–968.
- (40) Alsaiani, S. K.; Patil, S.; Alyami, M.; Alamoudi, K. O.; Aleisa, F. A.; Merzaban, J. S.; Li, M.; Khashab, N. M. *J. Am. Chem. Soc.* **2018**, 140, 143–146.
- (41) Chen, T.-T.; Yi, J.-T.; Zhao, Y.-Y.; Chu, X. J. *Am. Chem. Soc.* **2018**, 140, 9912–9920.
- (42) Xu, X.; Nan, D. Y.; Yang, H.; Pan, S.; Liu, H.; Hu, X. L. *Sens. Actuators, B* **2020**, 304, 127324.